Visible-Light Organic Photocatalysis for Latent Radical-Initiated Polymerization via 2e−/1H+ Transfers: Initiation with Parallels to Photosynthesis

Alan Aguirre-Soto,[†] Chern-Hooi Lim,[†] Albert T. Hwang,[†] Charles B. Musgrave,[†] and Jeffrey W. Stansbury*,[†,‡]

[†]Department of Chemical and Biological Engineering, University of Colorado Boulder, 3415 Colorado Ave., Boulder, Colorado 80303, United States

[‡]Department of Craniofacial Biology, School of Dental Medicine, University of Colorado, 12800 East 19th Ave., Aurora, Colorado 80045, United States

S *Supporting Information*

ABSTRACT: We report the latent production of free radicals from energy stored in a redox potential through a 2e−/1H+ transfer process, analogous to energy harvesting in photosynthesis, using visible-light organic photoredox catalysis (photocatalysis) of methylene blue chromophore with a sacrificial sterically hindered amine reductant and an onium salt oxidant. This enables light-initiated free-radical polymerization to continue over extended time intervals (hours) in the dark after brief (seconds) low-intensity illumination and beyond the spatial reach of light by diffusion of the metastable leuco-methylene blue photoproduct. The present organic photoredox catalysis system functions via a 2e−/1H+ shuttle

mechanism, as opposed to the 1e− transfer process typical of organometallic-based and conventional organic multicomponent photoinitiator formulations. This prevents immediate formation of open-shell (radical) intermediates from the amine upon light absorption and enables the "storage" of light-energy without spontaneous initiation of the polymerization. Latent energy release and radical production are then controlled by the subsequent light-independent reaction (analogous to the Calvin cycle) between leuco-methylene blue and the onium salt oxidant that is responsible for regeneration of the organic methylene blue photocatalyst. This robust approach for photocatalysis-based energy harvesting and extended release in the dark enables temporally controlled redox initiation of polymer syntheses under low-intensity short exposure conditions and permits visible-light-mediated synthesis of polymers at least 1 order of magnitude thicker than achievable with conventional photoinitiated formulations and irradiation regimes.
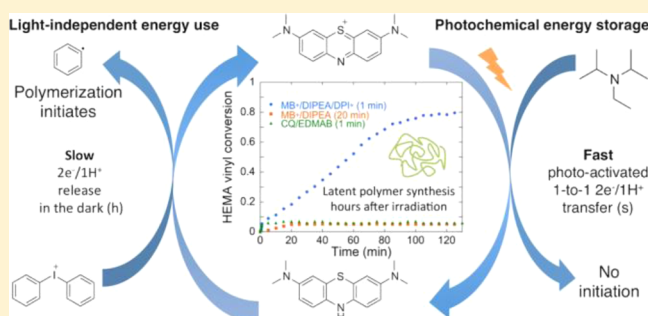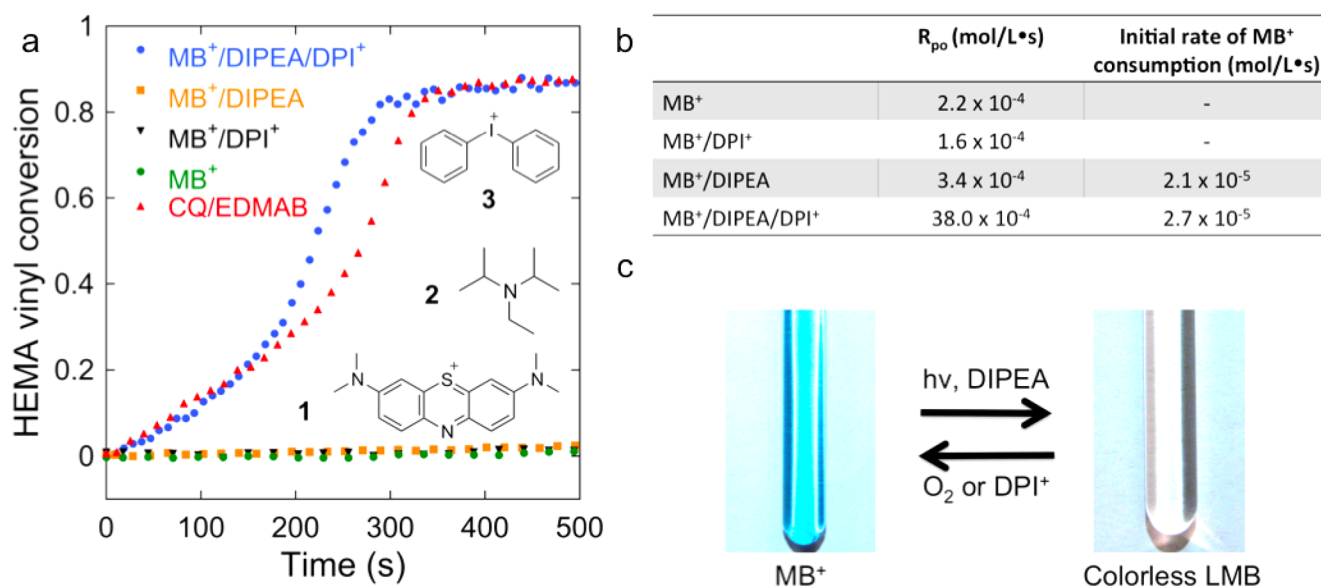
1. INTRODUCTION

Free radicals (radicals) participate in a wide variety of organic synthetic[1] and polymerization reactions,[2] e.g., vinyl homo- and copolymerizations,[3] thiol−ene click chemistry,[4] Cu-catalyzed azide−alkyne cycloadditions,[5] atom-transfer radical additions,[6,7] and alcohol to halide conversions.[8] Radical production by light activation provides unique temporal control of reactions. However, radicals must be produced continuously by large irradiation doses to sustain the balance between competing creation and termination of radicals. As a result, radical-initiated reactions characteristically halt quickly due to efficient radical termination when the external energy supply (light) is extinguished. Persistent or trapped radicals in dense polymer networks allow a limited degree of polymerization after light-cessation.[3,9] Whereas in controlled or "living" polymerization, the termination process is altered through an equilibrium that favors radicals in a dormant state so active radical concentrations remain low and essentially constant.[10,11]

However, living radical photopolymerization is usually slow and still requires continued irradiation.[10] Furthermore, no scheme has yet been devised to sustain radical production after the energy supply is extinguished without altering the radical termination process. Here, we report the first use of organic photoredox catalysis to continue radical production for extended time intervals in the dark after a brief initial low-intensity light exposure, opening new opportunities in photo-activated polymer and possibly organic synthesis.[12]

Conventionally, light-activated radical-based polymer synthesis entails radical production via photolytic bond cleavage, e.g., phosphine oxides or acetophenones,[13] or by light-mediated electron transfer or exchange between a chromophore, such as camphorquinone, and either a reductant or an oxidant.[14] In principle, radical generation in both of these approaches is

Figure 1. Evidence of radical production via photoredox catalysis of methylene blue (MB^+). (a) Conversion of vinyl group (polymerization) of 2-hydroxyethyl methacrylate (HEMA) during continuous irradiation of 1 mm thick samples. MB^+ (**1**)/DIPEA (**2**)/DPI^+ (**3**) are required for polymerization at a rate comparable to the conventional CQ/EDMAB formulation with the same amount of photons absorbed ($\sim$13 and 22 mW/cm^2, respectively). (b) Initial rates of polymerization (R_{po} from numerical differentiation of FT-IR data, see SI section 4) and initial rates of MB^+ bleaching (with UV−vis spectroscopy at $\sim$60 mW/cm^2). MB^+/DIPEA leads to efficient consumption of MB^+ (2.1×10^{-5} M/s) but no radical production (which correlates to the vinyl group conversion and R_{po}), whereas MB^+/DIEPA/DPI^+ increases radical production rate dramatically ($\sim$100-fold based on R_{po}) with no significant improvement on MB^+ consumption rate (2.7×10^{-5} M/s). Rates of bleaching without DIPEA are negligible. This indicates that DIPEA does not produce radicals efficiently (shows negligible polymerization). Thus, DPI^+ should play the main role in terms of radical production. (c) Photoredox cycle in methanol with DIPEA and O_2 or DPI^+. MB^+ in methanol is bleached, photoreduced to colorless LMB and regenerated by an oxidant. The process can be repeated as MB^+ is regenerated after each cycle, i.e., photocatalysis cycle.

restricted to where the excited molecules reside, i.e., within the imprint and penetration depth of photons. Examples of applications that rely on spatiotemporal controlled processing include the creation of patterned materials for nano- and microscale devices, metamaterials, laser imaging, and holography.[15−18] However, in optically thick materials, light absorption, scattering, and reflection limit light penetration and thus polymerization to mere millimeters, or often, to just tens to hundreds of micrometers from the irradiated surface while requiring high irradiation intensities or extended photocuring intervals.[19,20] As a result, through-plane polymerization is severely limited, which is detrimental in applications such as dental and orthopedic composites, irregular surface coatings, photolithographic resists, and cell-encapsulation hydrogels,[17,21−23] where unintentional property gradients and residual monomer beyond the light penetration depth limit is generally unacceptable. Ultimately, layer-by-layer polymerization is thus required if conventional free-radical photopolymer initiators are to be used for optically thick materials.

In contrast, radical generation through chemically activated redox initiation, such as with peroxide/amine combinations, allows synthesis of thick polymeric materials under ambient conditions upon *in situ* mixing of two-part formulations, as in bone cements.[24] However, this redox approach lacks temporal control of the initiation reaction beyond the mixing process. In other instances "dual-cure" systems require postirradiation heating or moisture cure.[25] "Dual-cure" systems, in which photo- and redox-activated chemistries work more or less simultaneously, introduce some temporal control. However, the two initiation modes work relatively independently, and mixing immediately prior to use is still required; thus, imposing similar temporal control limitations as redox systems.[26]

Frontal polymerization has been reported to allow deep shadow cure in free-radically and cationically initiated thick (centimeter scale) or opaque samples upon UV exposure.[27] Despite its attractive simplicity, limited storage stability of the peroxide-containing formulations and its inherent dependence on the self-propagated (by polymerization exothermicity) temperature wavefront (over 100 °C) have precluded the use of this technique in most applications.[28−30] No reports were found of free-radical photopolymerization of (meth)acrylates in which initiation extends beyond the irradiation space and time under ambient conditions without depending on the polymerization exotherm to sustain initiation in the dark.

In this contribution, we introduce the concept of organic photoredox catalysis as a novel approach to combine the temporal onset control of conventional photoactivation with the spatial reach of redox-activated radical production. We demonstrate that the combination of these phenomena extends the capabilities of prevailing photoinitiated processes and enables the practical synthesis of initially optically thick, centimeter-scale vinyl photopolymers at ambient conditions.

In recent years, photoredox catalysis has gained attention as an alternative to achieve faster rates of radical-initiated polymerization upon low-intensity visible-light irradiation.[31] Almost all of the reported mechanisms, including those for similar methylene blue (MB^+)/amine/onium salt formulations, rely on sequential $1e^-$ transfers to and from the photocatalyst, as is characteristic of ruthenium and iridium complexes.[31−38] In these mechanisms, transfer of a single electron allows production of (open-shell) radicals from the photoinduced electron-transfer (PET) step and essentially initiates the polymerization process immediately after the light-absorption event. Then, the consecutive $1e^-$ transfer step(s), responsible
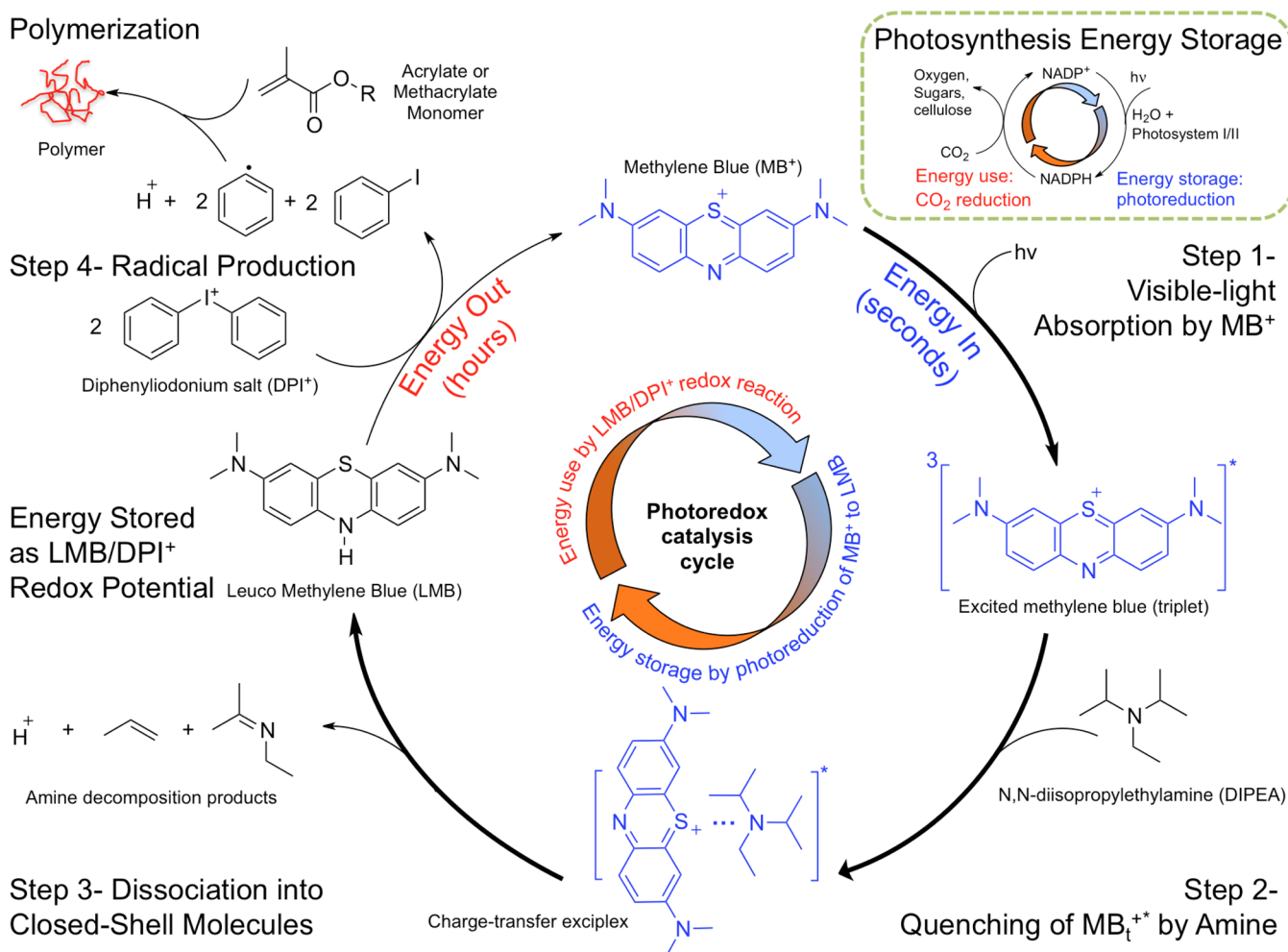
Figure 2. Free radical-initiated polymer synthesis with light energy harvesting cycle. Step 1: Visible-light ($h\nu$) excitation of MB^+ to the singlet state (not shown), which quickly decays to the longer-lived triplet state (MB_t^{+*}) via intersystem crossing. Step 2: Excess DIPEA quenches MB_t^{+*} to colorless LMB via transfer of two electrons and one proton (reaction 1) through formation of a charge-transfer excited-state complex (exciplex). Step 3: After a $2e^-/1H^+$ transfer, the exciplex separates into LMB and DIPEA-decomposition products. DIPEA decomposes to closed-shell molecules and does not initiate polymerization. Step 4: LMB is oxidized back to MB^+ by DPI^+ to produce two phenyl radicals per LMB. Phenyl radicals are responsible for the fast initiation of chain-growth polymerization of HEMA. Faster (thicker arrows) MB^+ reduction and slower (thinner arrows) reoxidation steps allow LMB to accumulate and also create a lag time between light absorption and radical generation. Thus, energy is stored as an electrochemical potential between LMB and DPI^+, which produces radicals beyond light absorption. This is analogous to the $NADP^+/NADPH$ cycle (inset) known in photosynthesis in which the transfer of $2e^-/1H^+$ in the photoredox cycle stores light energy in the form of a chemical potential that is used to reduce carbon dioxide to higher molecular weight sugars and carbohydrates.

for the regeneration of the photocatalyst, occur(s) so fast that light-energy "stored" in the photocatalyst as chemical energy is used shortly (less than a few seconds) after the PET step; thus these radical production approaches are incapable of sustaining the polymer synthesis for prolonged periods (hours) following light cessation.[10,33]

To the best of our knowledge, we report the first energy-harvesting approach using organic photocatalysis for latent light-induced radical-initiated polymer synthesis that relies on a two-electron/one-proton ($2e^-/1H^+$) transfer mechanism. Using a sterically hindered amine (N,N-diisopropylethylamine, DIPEA) as a sacrificial donor that induces a $2e^-/1H^+$ transfer to the organic photocatalyst MB^+ in a 1-to-1 fashion, we prevent immediate free-radical initiation of polymer synthesis of (meth)acrylate monomers upon light absorption and enable visible-light energy storage as chemical energy in a metastable closed-shell species: leuco-methylene blue (LMB). The stored energy is subsequently utilized to generate two initiating phenyl

radicals per photocatalytic cycle from the ground-state redox reaction between the metastable LMB and the oxidizer (diphenyliodonium, DPI^+) for extended time intervals (hours) after short, low-intensity irradiation.

Using photocatalysis to store light-energy in a metastable species (via a $2e^-/1H^+$ transfer mechanism) in order to sustain ground-state reactions (e.g., radical generation that initiates polymer synthesis) for extended periods (hours) after a brief light activation is the basis of the approach presented herein. Similar PET-based mechanisms have been envisioned as the basis for 'molecular circuits' and 'molecular computing devices',[39,40] but we present the first example of a PET-based scheme for light harvesting analogous to photosynthesis that allows photopolymerization be extended well beyond irradiation. In this paper, we: (1) describe coupled experimental and quantum chemical studies that support the photoinduced redox radical formation via the $2e^-/1H^+$ transfer mechanism and (2) demonstrate the capabilities of this new radical production

approach within the scope of radical chain-growth polymer synthesis.

2. RESULTS AND DISCUSSION

2.1. Fast Radical Production in MB⁺/DIPEA/DPI⁺ Formulations. Radical production was analyzed by monitoring the disappearance of the infrared absorption corresponding to the vinyl group (=CH₂) of the monomer with Fourier transform near-infrared spectroscopy (FT-NIR).[41] The extent of vinyl group consumption indicates monomer conversion due to polymerization, which correlates with radical production. Under continuous, low-intensity visible-light irradiation, monomer solution (e.g., 2-hydroxyethyl methacrylate; HEMA) containing methylene blue (MB⁺, **1**), N,N-diisopropylethylamine (DIPEA, **2**), and diphenyliodonium cation (DPI⁺, **3**) reaches a vitrification-limited 85% conversion in 500 s (Figure 1a). Under the same conditions, formulations where either or both DIPEA and DPI⁺ are absent (MB⁺/DIPEA; MB⁺/DPI⁺; or MB⁺) exhibit less than 2% monomer consumption.

To further probe the initiation process, the concentration of MB⁺ was analyzed via real-time ultraviolet−visible (UV−vis) spectroscopy. MB⁺ is consumed efficiently (Figure 1b) in the presence of DIPEA with or without DPI⁺. However, the MB⁺/DIPEA formulation is ineffectual toward initiating polymerization, whereas the MB⁺/DIPEA/DPI⁺ formulation leads to a significant radical production rate, as demonstrated by HEMA conversion, that is comparable to the reaction kinetics and conversion achieved with a conventional visible-light initiator composed of camphorquinone (CQ) and ethyl 4-dimethylaminobenzoate (EDMAB), for which equivalent amounts of photons are absorbed (Figure 1a and see the Experimental Section). Hence, direct radical production from MB⁺ consumption by DIPEA is negligible. This indicates that MB⁺ consumption and radical production involve separate reaction steps (described in detail in Sections 2.2 and 2.3); while MB⁺ consumption is primarily dependent on the presence of DIPEA; the oxidant (DPI⁺) plays the main role in radical production.

2.2. PET Reaction of MB⁺/DIPEA Generates the Colorless LMB. Now, we reevaluate the MB⁺/DIPEA system to establish the connection between photoreduction of MB⁺ and the subsequent radical generation that necessitates the presence of DPI⁺. In general, the reduction of MB⁺ has been proposed to proceed via a 2e⁻/1H⁺ process to produce the leuco product LMB in a reducing environment,[42,43] as represented in reaction 1.

$$MB^+ + 2e^- + 1H^+ = LMB \qquad (1)$$
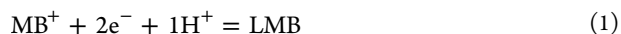
Under irradiation, the 2e⁻/1H⁺ transfer process (reaction 1) is driven by light and is referred to as PET.[44,45] The PET of specific interest here is the reduction of MB⁺ to the colorless LMB in the presence of DIPEA (reductant). For example, in Figure 1b, we see that the rates of MB⁺ consumption for the MB⁺/DIPEA and MB⁺/DIPEA/DPI⁺ formulations are 2.1 × 10⁻⁵ and 2.7 × 10⁻⁵ M/s, respectively. Reduction of MB⁺ to LMB is identified by the decrease of the ~650 nm centered peak and appearance of a ~250 nm centered peak (Figure 1b and see SI section 7). This process is commonly known as "photobleaching", where the signature blue color of MB⁺ (λ_{max} = ~650 nm) disappears and the mixture turns colorless (Figure 1c).

Next, we describe the PET process in greater detail, as illustrated in Figure 2. In step 1, absorption of photons excites MB⁺, which undergoes intersystem crossing to ultimately produce the triplet excited-state MB$_t^+$*. Subsequently in step 2, an excited-state complex (exciplex) forms between DIPEA and MB$_t^+$* prior to the PET reaction.[46] It is important to note that in conventional PET reactions involving amines and chromophores, the amine reductant typically provides one electron (e⁻) and one proton (H⁺) to the photoexcited chromophore.[32−34,44,45,47] For example, with the CQ chromophore and EDMAB reductant, transfer of 1e⁻/1H⁺ results in the production of the alpha-aminoalkyl radical that is reactive toward vinyl monomers and thus initiates polymerization.[38,48] If the analogous 1e⁻/1H⁺ transfers occur in MB⁺/DIPEA photoreduction, two DIPEA molecules would be required for each bleached MB⁺ (reaction 1). As a result, each amine would result in an alpha-aminoalkyl radical that would be expected to cause fast polymerization of the methacrylate monomer. Quantum chemical simulations predict that creation of a monomer-based radical with the alpha-aminoalkyl radical, i.e., initiation of the polymerization, is barrierless and thus confirms that polymerization would be fast and diffusion-limited in solution if DIPEA-based radicals were produced. In Figure 3,
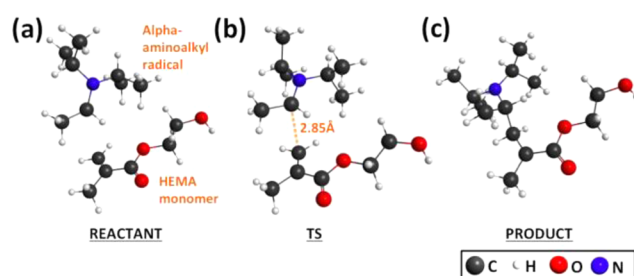
Figure 3. Reaction between alpha-aminoalkyl radical and HEMA monomer. Equilibrium structures of (a) reactant, (b) TS, and (c) product are determined using unrestricted M06/6-311G(d,p)/CPCM-methanol. The enthalpic barrier for this reaction is determined to be ΔH^0_{act} = −1.4 kcal/mol, after zero-point-energy (ZPE) and thermal corrections to 298 K. Note that although ΔE^0_{act} is positive, thermal and zero-point corrections often produce a negative ΔH^0_{act} for reactions that are essentially barrierless.

we show the equilibrium structures of (a) reactant, (b) transition state (TS), and (c) product for the C−C bond formation reaction between the alpha-aminoalkyl radical and HEMA monomer.

Despite the formation of LMB, we observed no significant polymerization with MB⁺/DIPEA (Figure 1a). This contrasts with other tertiary aliphatic amines that photoreduce MB⁺ via 1e⁻/1H⁺ transfers to produce alpha-aminoalkyl radicals that initiate polymerization efficiently, as previously reported[37,49,50] and confirmed by our FT-NIR spectroscopy measurements with other tertiary amines (SI, section 2). This observation compelled us to propose that the strong and sterically hindered DIPEA base plays a unique role in the MB⁺ PET reaction examined here: it reacts rapidly with the photoexcited MB$_t^+$* in a 1-to-1 fashion, where DIPEA serves as a 2e⁻/1H⁺ donor. Hence, closed-shell degradation products are produced from the PET reaction (Figure 2, step 3) but not DIPEA-based (alpha-aminoalkyl) radicals. Using electrospray ionization-mass spectrometry (ESI⁺), we identified both 2-ethyliminopropane and propene as the byproducts of the entropy-driven DIPEA

decomposition via carbon–nitrogen σ-bond cleavage (SI, section 3).

To our knowledge, this is the first time a $2e^-/1H^+$ transfer mechanism has been demonstrated for the photoreduction of a photocatalyst (MB$^+$) with an amine (DIPEA) in 1:1 ratio that produces no alpha-aminoalkyl radicals during the PET reaction.

Finally, the PET reaction in step 3 leads to the desired LMB product. Examination of the calculated LMB equilibrium structure (Figure 4) suggests that a dearomatization process
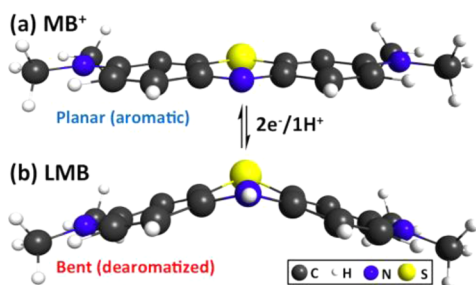
Figure 4. Dearomatization of MB$^+$ after a $2e^-/1H^+$ transfer. (a) MB$^+$ is a planar aromatic molecule that absorbs strongly in the visible light spectrum ($\lambda_{max} = \sim650$ nm). (b) LMB is a photoproduct of a $2e^-/1H^+$ transfer in MB$^+$/DIPEA PET reaction. After a $2e^-/1H^+$ transfer, the thiazine ring in LMB is dearomatized and is significantly bent from the original planar structure. Time-dependent DFT (TD-DFT, Experimental Section) using ωB97XD/LANL2dz/CPCM-methanol predicts that LMB absorbs at $\lambda_{max} = \sim300$ nm, which corroborates the observed blue-shift of λ_{max} to ~250 nm and explains the bleaching of the solution to its colorless form.

occurs after $2e^-/1H^+$ transfer (reaction 1), where the thiazine ring distorts significantly from its original planar structure. Furthermore, excited-state calculations using TD-DFT predict

that the PET process significantly blue-shifts MB$^+$ absorption, which is typical of a dearomatization process. LMB is predicted to absorb only in the near-UV region at ~300 nm (compared to ~650 nm for MB$^+$), which agrees with the appearance of the ~250 nm peak during PET. Next, we examine how LMB, a metastable closed-shell product from PET, participates in a ground-state reaction with the DPI$^+$ oxidant to generate the radicals responsible for polymerization.

2.3. Radical Production From LMB/DPI$^+$ Reaction. If photoreduction of MB$^+$ by DIPEA produces LMB by reaction 1 but generates no radicals, then the radicals responsible for the fast polymerization of the monomer with MB$^+$/DIPEA/DPI$^+$ must arise from the ground-state oxidation of LMB back to MB$^+$ by DPI$^+$. This proposal is based on the fact that LMB has been observed to oxidize to MB$^+$ with O$_2$ as the oxidant, consistent with the observed gradual return of MB$^+$'s blue color (Figure 1c). Furthermore, LMB is an efficient reducing agent.[37,51−53] Herein we propose that radical production in MB$^+$/DIPEA/DPI$^+$ (Figure 2, step 4) occurs as follows:

$$LMB + 2DPI^+ = MB^+ + 2Ph^\bullet + 2I{-}Ph + H^+ \qquad (2)$$

DFT calculations performed at the uM06/6-311G**// uωB97XD/LANL2dz level of theory in CPCM implicit methanol solvent (see Experimental Section) support reaction 2 with a predicted ΔG^0_{rxn} of −5.2 kcal/mol. Furthermore, production of two highly reactive phenyl radicals per LMB accounts for the fast polymerization rate observed with MB$^+$/DIPEA/DPI$^+$ (Figure 1a) under irradiation. ESI$^+$ shows the production of iodobenzene-based products (SI, section 3), which provides additional evidence for (reaction 2); the oxidation of LMB by DPI$^+$ via (reaction 2) also explains the observed return of MB$^+$'s blue color.

To further investigate the radical generation process described by reaction 2, we performed an Arrhenius analysis
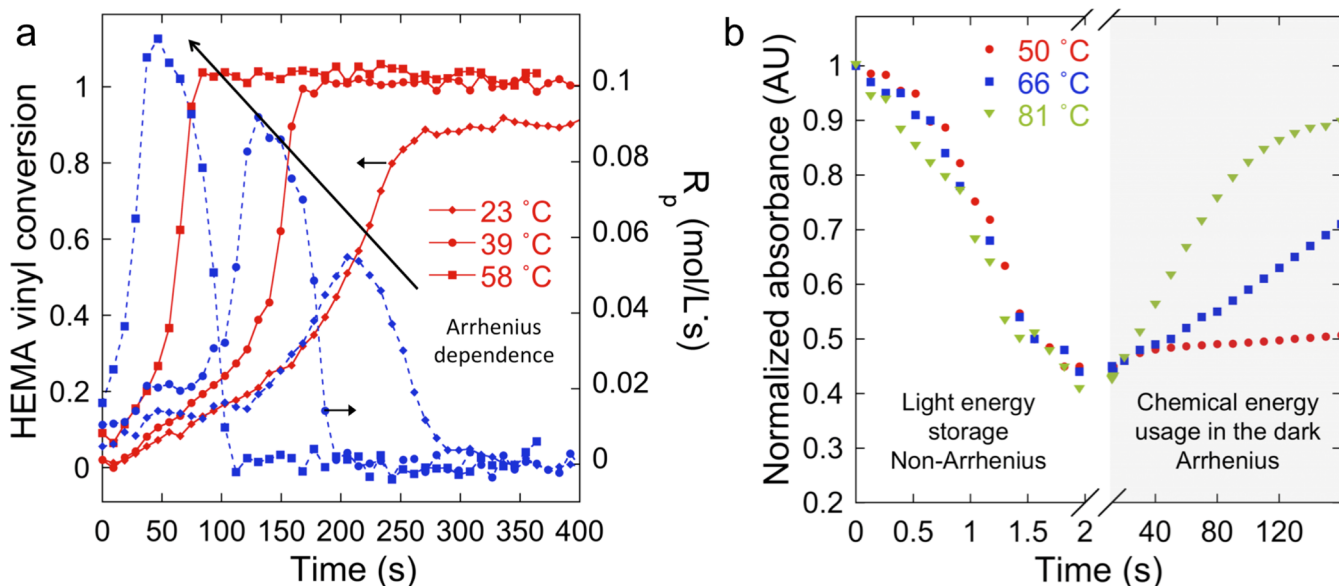
Figure 5. Activation energy for MB$^+$ regeneration matches initiation of polymerization. (a) Vinyl conversion (red continuous line) and R_p (blue dashed line-obtained from numerical differentiation of FT-IR data) under illumination show Arrhenius (temperature) dependence. Activation energy for initiation of polymerization ($\Delta E_{act} = 6.6 \pm 1$ kcal/mol) is due to the redox reaction between LMB and DPI$^+$ (arrows indicate temperature increase). (b) Absorbance monitoring (650 nm, MB$^+$ peak) proves temperature-insensitive (light-dependent) photoreduction of MB$^+$ by DIPEA, i.e., bleaching of the blue color. After 10 s of irradiation, MB$^+$ is regenerated in the absence of light. Activation energy for MB$^+$ regeneration ($\Delta E_{act} = 7.2 \pm 1.2$ kcal/mol) agrees with the estimated activation energy for the initiation of polymerization (from FT-NIR) because both are due to the LMB/DPI$^+$ reaction.
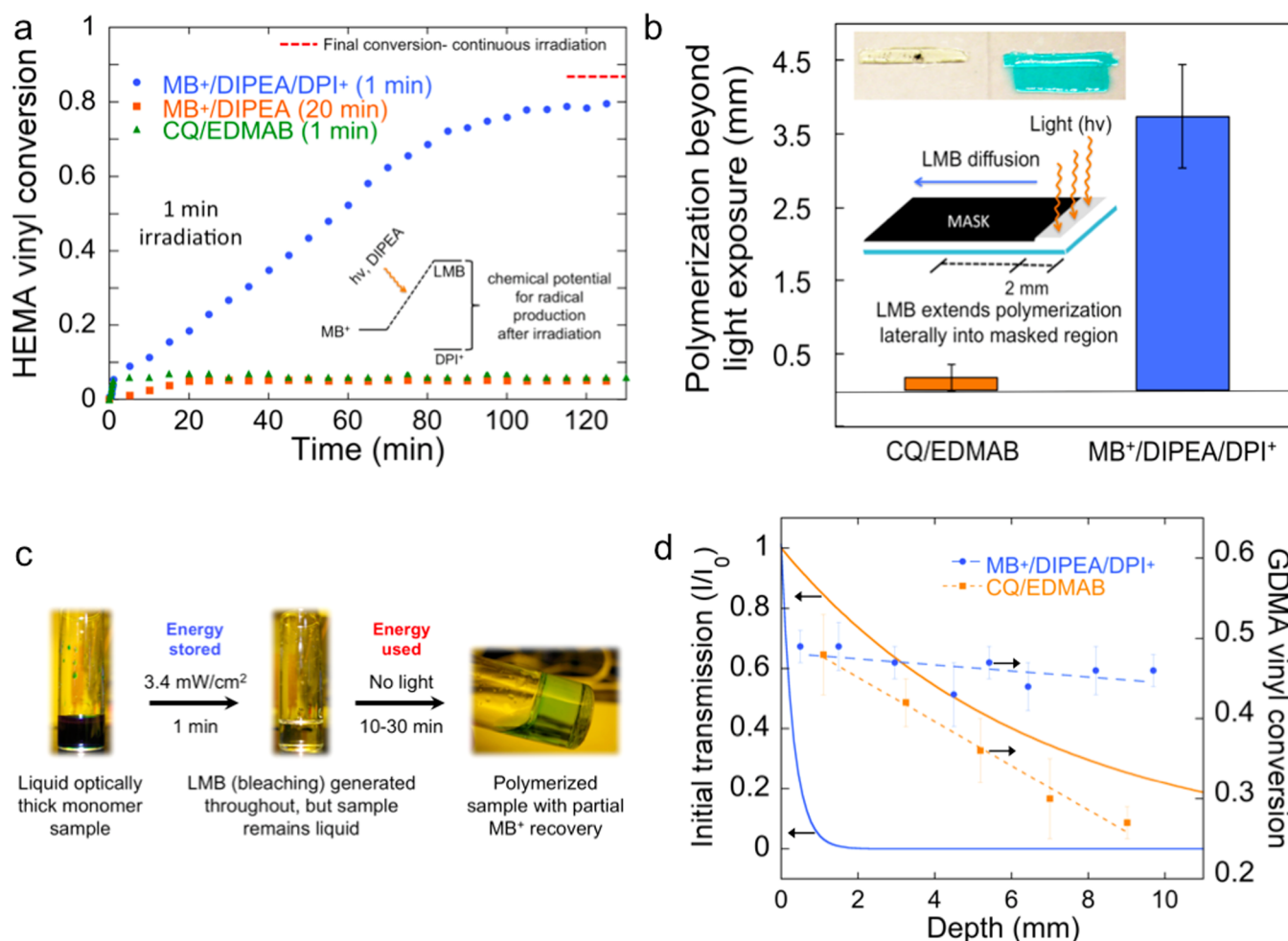
Figure 6. Radical generation in the dark from stored energy in LMB. (a) HEMA with MB$^+$/DIPEA/DPI$^+$ reaches 80% conversion with 60 s of illumination after having achieved only 8% conversion during active irradiation. MB$^+$/DIPEA and CQ/EDMAB show no energy-harvesting capability. (b) Stable LMB diffuses and extends radical production beyond the light absorption site. Polymerization is initiated into a masked region 3.7 ± 0.7 mm (standard deviation, $n = 3$) away from the illuminated region (2 mm in width) with MB$^+$/DIPEA/DPI$^+$. Statistically negligible extension of polymerization was observed in the masked region with CQ/EDMAB at equivalent conditions. (c) Polymerization of optically thick 1.2 cm (height) HEMA and GDMA. Poly-HEMA discs were made with 1 min irradiation (from the top). An analogous sample with CQ/EDMAB was irradiated with an equivalent number of absorbed photons showing negligible polymerization and remained liquid (SI section 5). (d) Vinyl conversion by FT-NIR (with standard deviation, $n = 3$) is more uniform throughout the depth in a 10 times more optically opaque MB$^+$/DIPEA/DPI$^+$ sample than in a conventional CQ/EDMAB sample. Dashed lines indicate the linear regression of the final conversion profile, and solid lines indicate the local light transmission profile at the start of irradiation (based on the respective active wavelengths and molar absorptivities of CQ and MB$^+$ in GDMA).

to determine that the activation barrier for the free radical production step in the polymerization of HEMA with MB$^+$/DIPEA/DPI$^+$ is $\Delta E_{act} = 6.6 \pm 1.0$ kcal/mol (Figure 5a and SI, section 3). Next, we used real-time UV−vis to quantify the regeneration rate of MB$^+$ at various temperatures after a 10 s irradiation (Figure 5b). We observed that light-activated MB$^+$ consumption is temperature independent (Figure 3b, light), as expected for a PET reaction where diffusion restrictions are mitigated by excess reductant (DIPEA). In contrast, MB$^+$ regeneration is strongly temperature sensitive (Figure 5b, shaded). From the UV−vis results, we estimate that ΔE_{act} for MB$^+$ regeneration is 7.2 ± 1.3 kcal/mol (SI, section 4).

Statistical agreement in ΔE_{act} values from independent Arrhenius analyses of both monomer consumption and MB$^+$ regeneration effectively confirms that the two observations are due to reoxidation of LMB by DPI$^+$. Notably, there is an alternative radical production pathway based on direct redox reaction between DIPEA and DPI$^+$; however, its ΔE_{act} is $13.1 \pm$

1.0 kcal/mol (SI, section 4). From this we calculate that well over 90% (depending on MB$^+$/DIPEA/DPI$^+$ concentrations) of the phenyl radicals originate from the LMB/DPI$^+$ reaction once LMB is generated via MB$^+$ photoreduction.

2.4. Stored Energy in LMB Extends Radical Production after Irradiation. Having demonstrated that this photocatalysis mechanism most likely proceeds via a $2e^-/1H^+$ transfer, we now show that MB$^+$/DIPEA/DPI$^+$ can be tuned so that the polymerization reaction continues for hours after light cessation. In Figure 6a, we show that during a 1 min low-intensity light exposure, the bulk polymerization of HEMA reached ∼8% conversion for MB$^+$/DIPEA/DPI$^+$. Extinguishing the irradiation at this point led to the continued rise in conversion in the dark over the next 2 h to reach 80%, with radical formation likely persisting over even longer time scales. This offers additional proof that the above-described radical production by LMB/DPI$^+$ occurs via a ground-state "dark" reaction. Similar studies with additional irradiation times are

7423

dx.doi.org/10.1021/ja502441d | *J. Am. Chem. Soc.* 2014, 136, 7418−7427

provided in SI section 5 to confirm this unique behavior. The initial PET reaction "charges" the photocatalytic cycle by quickly converting MB^+ into LMB via steps 1−3 of Figure 2, also demonstrated in Figure 3b. The sample bleaches as LMB accumulates because step 4 (or equivalently reaction 2) is rate limiting. Light energy is subsequently harvested as the chemical potential between MB^+ and LMB, and "dark" reaction with DPI^+ drives radical production and polymerization after the brief PET reaction. In contrast, polymerization did not continue in the dark for MB^+/DIPEA or CQ/EDMAB in HEMA. It is noteworthy that the final "dark" conversion achieved with MB^+/DIPEA/DPI^+ is nearly the same as that obtained with continuous light exposure (86%, Figure 1a), which indicates the final conversion is not significantly hampered by such a short initial light exposure period.

2.5. Photocatalysis Cycle Mimics Photosynthesis. The photoredox catalysis here mimics nature's photosynthesis where energy from visible light is stored as the chemical potential in the MB^+/LMB redox couple. This is analogous to photosynthesis, where visible-light absorbing proteins in Photosystems I and II undergo PET reactions to store energy in the $NADP^+$/NADPH redox couple. Both redox couples store energy using a $2e^-/1H^+$ transfer reaction and participate in ground-state (light-independent analogous to the Calvin cycle) reactions to release the stored energy. While the closed-shell NADPH energy carrier drives the synthesis of sugars and natural polymers in the absence of light;[54,55] the system utilizes its stored energy, originally derived from light, in LMB to generate radicals (reaction 2) that initiate polymerization for the synthesis of macromolecules in the absence of light.

2.6. Spatial Extension of Radical Production beyond the Irradiation Site. Next, we demonstrate that polymer synthesis with MB^+/DIPEA/DPI^+ not only extends temporally but also spatially beyond the reach of photons (Figure 6b). HEMA was polymerized on a glass substrate by exposing the unmasked 2 mm fringe of an 8 mm long monomer sample to continuous irradiation for 10 min. The lateral extent of photoactivated polymerization into the shadowed region was determined by washing away unreacted monomer with acetone after 30 min of storage in the absence of light. CQ/EDMAB yielded a patterned polymer that extended only $170 \pm 190 \ \mu m$ into the masked region (Figure 6b, islet). Notably, during this time, the MB^+/DIPEA/DPI^+ formulation shows 3.73 ± 0.73 mm of lateral polymerization into the dark area. This is due to relatively stable LMB produced in the irradiated region (reaction 2) diffusing into the masked region and reacting with DPI^+; thus, generating radicals and initiating polymerization "far" (millimeters) from the LMB-formation site. Using embedded thermocouples, we verified that there is no thermal front involved in the extension of polymerization beyond the direct light activation.[56] While many photopolymer applications rely on the intrinsic spatial control associated with conventional photoinitiating systems, this approach uniquely decouples spatial restrictions from the photoactivation process. It is certainly advantageous in instances where radical generation around corners and into shadowed regions is desirable, such as in automotive and aerospace coatings of irregular surfaces and polymers for *in situ* biomedical applications.

2.7. Photoactivated Synthesis of Thicker Polymers. The aforementioned temporal and spatial extension of radical generation is utilized to achieve light-mediated synthesis of polymers at least an order of magnitude thicker than the millimeter-scale of conventional photoinitiated formulations

under low-intensity and short exposure conditions. The full depth of ~1.2 cm thick HEMA polymer specimens (Figure 6c) was photocured with a 1 min exposure to 3.4 mW/cm² light. Under these very mild conditions, the photoreduction of MB^+ to LMB initially occurs near the top surface, close to the irradiation source, where photon flux is highest. As MB^+ is transformed into LMB, bleaching occurs in a gradient fashion allowing the light to penetrate deeper into the originally optically thick sample. Within 1 min of illumination the sample is entirely colorless but not yet polymerized. HEMA polymerization then continued in the dark using the radicals from the LMB/DPI^+ reaction. After 30 min, the sample was gelled throughout with polymerization continuing to completion in the dark over several hours.

Due to diffusion constraints in the polymer, the blue color in the polymer does not fully regenerate, as not all LMB is able to oxidize to MB^+. The multimillimeter diffusion of the relatively stable high-energy close-shell LMB (Figure 4b) can aid in achieving centimeter plus-scale polymerization even if MB^+ photobleaching were not complete throughout the entire depth of the sample. For instance, CQ transmits more light through the 1.2 cm samples and can be bleached efficiently with EDMAB allowing for progressive light penetration in the same sample geometry; however, CQ/EDMAB specimens show noticeably less polymerization at equivalent photon absorption, i.e., essentially no polymerization of HEMA at these mild conditions (SI section 6).

These capabilities can also be exploited with other monomers, such as the cross-linking photopolymerization of glycerol dimethacrylate (GDMA) or triethylene glycol di-(meth)acrylate. The higher modulus GDMA polymer was used to prepare similarly thick samples, which were then sectioned (~1 mm slices) to reveal a much more uniform conversion profile to a depth of at least 1 cm, than what is achieved with the analogous CQ/EDMAB sample, which has an initially 10-fold greater optical transparency (Figure 6d). The limiting GDMA conversion (~65%) is achieved in the top layer with either initiator system with an equivalent amount of photons absorbed. However, it is remarkable that conversion in the MB^+/DIPEA/DPI^+ system reduces only marginally (~5%) at a depth of 1 cm under such mild irradiation conditions, while conversion in the CQ/EDMAB formulation drops precipitously to zero, as is typical for conventional radical-initiated photopolymerizations. In general, much higher intensities and/or longer exposures are needed to achieve this same outcome with conventional photoinitiators as demonstrated using CQ/EDMAB.

Such a small variation in monomer vinyl conversion with depth permits the design of photoactivated initiation systems for synthesis of optically thick polymers under milder, highly energy-efficient irradiation regimes and within a time scale comparable to conventional redox initiators,[57] but with unprecedented temporal activation control. We contend that this is the first photoredox catalysis employed to design a temporally controlled redox initiation system where the active radicals are not generated directly by the light-dependent reaction, and in which the rates of photoreduction and oxidation in the photoredox cycle can be tuned to achieve energy storage that extends polymerization well beyond the time and distance associated with the light absorption process.

3. CONCLUSIONS

The key to extend initiation beyond irradiation with this photoredox catalysis concept is achieving a fast, efficient photochemical storage step (photobleaching), in which light energy is converted into chemical energy and later released in a much longer time interval based on the chemical potential of the redox pair (e.g., LMB/DPI$^+$). The energy utilization on much longer time scales than that of light absorption is tuned by the kinetics of the ground-state redox reaction. Thus, the primary reason for the use of DIPEA as the reductant in the presented system is its fast bleaching "rate" with MB$^+$ and the lack of alpha-aminoalkyl radical formation. This approach unlocks new opportunities for the application of other chemistries that enable energy storage in bulk and solution polymer and possibly organic synthesis.[1]

The concentration of MB$^+$, and the associated LMB, will affect the rate (kinetics) and duration (thermodynamics) of the polymerization after the short light pulse. The experimental parameters used herein were not optimized, and we expect that this concept can be improved to synthesize even thicker polymers. This work serves only as proof of concept for the novel initiation scheme and can be extended to a range of polymer applications and likely organic synthesis as well.

Ruthenium and iridium complexes produce photoexcited states that are a more powerful source of electrochemical potential,[12] which may allow for greater potential, however different sacrificial reductants or oxidants would be required to allow analogous storage of energy derived from light and to avoid initiation shortly after the light-absorption event. Ultimately we propose that additional organic and organometallic photocatalysis schemes can be engineered to delay light-energy utilization to hours after light absorption by appropriate formulation design. Photoredox organocatalysis is an attractive alternative for any synthetic applications in which expensive photocatalysts (i.e., organometallic) cannot be recovered, as would be the case in bulk polymerizations. Additionally, organic photocatalysts are more versatile, lower-cost, and usually less toxic alternatives.

This concept could provide significant advantages, including photopolymerization of optically thick UV-absorbing monomer formulations, in wide ranging industrial and biomedical applications, such as cell encapsulation, orthopedic and dental cements, tumor phototherapy, adhesives, and high-throughput polymer films. The final blue tone of the polymer films and discs varied with irradiation dose and initial concentrations. However, if desired, the reformed MB$^+$ and the blue color can be partially or completely removed from most polymers by swelling, as seen in SI section 7, depending on cross-linked density of the polymer network.

4. EXPERIMENTAL SECTION

Materials. Methylene blue (MB$^+$), *N,N*-diisopropylethylamine (DIPEA), and diphenyliodonium chloride salt (DPI-Cl) were used as received. 2-Hydroxyethyl methacrylate (HEMA) and glycerol dimethacrylate (GDMA) were selected as monomers because they readily dissolve MB$^+$/DIPEA/DPI$^+$. Homogeneous samples were prepared by vortex mixing. Methanol (MeOH), acetonitrile (ACN), and DI-water were used as solvents (spectro grade). All materials were commercially obtained from Aldrich (Milwaukee, WI) and used as received.

Light Source. A halogen dental curing light (Max, DENTSPLY/Caulk, Milford, DE) modified to deliver broadband 500−800 nm light was used in the MB$^+$/DIPEA/DPI$^+$ photopolymerization experiments. Incident irradiance was measured with a radiometer (6253, Interna-

tional Light Technologies, Peabody, MA) within the 400−700 nm range, i.e., not all of which is absorbed by MB$^+$. For all the CQ/EDMAB-initiated formulations, the 400−500 nm output of an unaltered halogen lamp was applied with the incident irradiance verified by radiometer.

FT-IR. Bulk polymerizations of HEMA were monitored in real-time with a FT-near-IR spectrophotometer (Nicolet Magna-IR Series II, Thermo Scientific, West Palm Beach, FL) by following the peak area of the first overtone absorption band for the methacrylate ═CH$_2$ group (6167 cm^{-1}). The spectrophotometer was equipped with a KBr beam splitter, a MCT/A detector, and an in-house fabricated horizontal stage adapted for *in situ* photopolymerization experiments.[41] The distance between the light source and the sample was ∼7 cm to ensure uniform irradiation across the entire sample with controlled irradiance values. An 800 nm cutoff filter was used to eliminate the 633 nm HeNe reference beam within the NIR output signal. The sample holder for the *in situ* polymerization, both in the dark and in the light, consisted of a 1 mm height, 1.6 cm diameter disc fabricated by interjecting a perforated silicone rubber shim in between two 1 mm thick glass slides. Rate of polymerization was calculated by numerically differentiating the peak area as a function of time. Concentrations used were as follows: [MB$^+$] = 4 mM, [DIPEA] = 0.2 M, [DPI$^+$] = 0.04 M, [CQ] = 0.02 M, and [EDMAB] = 0.04 M. All FT-NIR-monitored polymerizations with MB$^+$/DIPEA/DPI$^+$ were performed with 12−13 mW/cm^2. For the CQ/EDMAB system the intensity used was 22−23 mW/cm^2. These intensities gave an approximate 3 × 10^{-8} Einsteins/s·cm^2 of photons absorbed in both systems based on differences in molar absorptivities and concentrations of the MB$^+$ and CQ species.

UV−vis (electronic) Spectroscopy. A diode array spectrophotometer (Evolution 300, Thermo-Scientific, West Palm Beach, FL) was employed. Absorbance spectra were collected in quartz cuvettes with a 1 cm path length (l). FT-NIR samples were also employed to remotely monitor MB$^+$ bleaching in real-time by UV−vis in the same horizontal stage but separately from the IR experiments. Concentrations used were as follows: [MB$^+$] = 4 mM, [DIPEA] = 0.2 M, and [DPI$^+$] = 0.04 M. UV−vis experiments were performed with an intensity of 60 mW/cm^2 to accelerate the bleaching rate of MB$^+$ and avoid significant polymer diffusion constraints to the reoxidation reaction between LMB and DPI$^+$.

Electrospray Ionization Mass Spectrometry (ESI-MS). Identification of the intermediates and final products of the reaction was performed in a LC/MS/MS mass spectrometer system (ABI 4000 Q TRAP, Life Technologies, Carlsbad, CA) equipped with a triple quadruple/linear ion trap analyzer and ESI detection.

Quantum Chemical Calculations. Excited-state calculations were performed using TD-DFT with the uωB97XD[58]/6-311G** level of theory where solvation in methanol was described using a polarizable continuum model (CPCM).[59] The reaction between an alpha amino-alkyl radical (derived from DIPEA) and HEMA monomer was determined to be barrierless, where the calculations were performed using uM06[60]/6-311G**/CPCM-methanol. In predicting the thermochemistry in reaction 2, we employed uM06/6-311G**// uωB97XD/LANL2dz in CPCM described methanol solvent. To estimate the entropy contribution to the free energy, a frequency calculation was performed using uωB97XD/LANL2dz. All calculations were performed using the GAUSSIAN09[61] and GAMESS[62] computational chemistry software packages.

Lateral Polymerization Experiments. Experiments were performed in a J500 Mask Aligner from Optical Associates. Exposed monomer borders a 500 μm thick opaque rubber spacer on all sides such that photogenerated molecules can diffuse only in one direction. The exposed fringes were 2 × 18 mm, and the total monomer samples were 8 × 18 mm. Light intensity was chosen so R_p is equal in the MB$^+$/DIPEA/DPI$^+$ and CQ/EDMAB initiating systems, hence achieving ∼80% conversion during the 10 min irradiance in both cases, i.e., diffusion restrictions are roughly equivalent. The use of a collimated light beam and a nonreflective surface prevented light from reflecting into the masked region from the exposed region of the sample. A black mask was used as a substrate at the bottom of the

samples to eliminate any reflectance of photons into the masked region. A glass microscope slide was used as the top boundary to be able to obtain final polymer samples that adhered to the glass. Concentrations used were as follows: $[MB^+] = 0.4$ mM, $[DIPEA] = 0.2$ M, $[DPI^+] = 0.04$ M, $[CQ] = 0.02$ M, and $[EDMAB] = 0.04$ M. Light intensity used was 12 mW/cm^2 for the MB$^+$/DIPEA/DPI$^+$ system and 23 mW/cm^2 for the CQ/EDMAB system to obtain approximately equivalent amounts of absorbed photons.

Thick Disc Polymerization Experiments. MB$^+$/DIPEA/DPI$^+$ and CQ/EDMAB samples were prepared in HEMA. Monomer (1.5 mL) with each initiator in glass vials was irradiated for 1 min at 3.4 mW/cm^2 (>500 nm) for MB$^+$/DIPEA/DPI$^+$ and 6.6 mW/cm^2 (400–500 nm) for CQ/EDMAB to achieve equivalent photon absorption. Samples were then stored in a closed container with no light access for over 30 min. The progression of the viscosity of the samples was periodically monitored in both cases qualitatively and photographed. Concentrations used in these experiments were as follows: $[MB^+] = 0.4$ mM, $[DIPEA] = 0.2$ M, $[DPI^+] = 0.04$ M, $[CQ] = 0.02$ M, and $[EDMAB] = 0.04$ M. At these conditions the HEMA with CQ/EDMAB remains liquid and cannot be sectioned for FT-NIR analysis. Thus, additional experiments with GDMA were performed using 9–10 mW/cm^2 for MB$^+$/DIPEA/DPI$^+$ and 17–18 mW/cm^2 for CQ/EDMAB. At these intensities, the ~1.2 cm thick samples were sectioned to ~1.5 mm slices, which were analyzed with FT-NIR after 60 s irradiation and 90–120 min in dark storage. To determine conversion means and standard deviations as a function of depth, the experiments were repeated 3–4 times. All samples were purged with nitrogen for 5 min before irradiation at a pressure of 10–20 psi.

Methylene Blue Extraction from Poly-HEMA Gel. A 1.2 × 1.1 cm poly-HEMA disc was polymerized from bulk HEMA (97%) with MB$^+$/DIPEA/DPI$^+$ using 5 min irradiation at 11 mW/cm^2 of a white LED lamp. The sample was left to react in the dark for 30 min. Then, the polymer gel was removed from the mold and introduced into 20 mL of water. UV–vis absorbance of the water solution was monitored with time to track the change in the peak at ~660 nm, indicative of the MB$^+$ concentration in solution.

ASSOCIATED CONTENT

Supporting Information

Quantum Chemical Calculations and Coordinates of Molecular Structures for reaction between DIPEA-based alpha amino alkyl radical and HEMA monomer. HEMA vinyl conversion with MB$^+$ and DIPEA, MDEA or TEA. ESI$^+$ spectra for photo-reaction of MB$^+$/DIPEA and MB$^+$/DIPEA/DPI$^+$ in methanol. Activation energy calculations and plots. HEMA vinyl conversion with MB$^+$/DIPEA/DPI$^+$ for several irradiation doses. Photograph of liquid CQ/EDMAB sample in HEMA after irradiation. UV–Vis spectra for water solution with MB$^+$ after swelling of HEMA gel. This material is available free of charge via the Internet at http://pubs.acs.org.

AUTHOR INFORMATION

Corresponding Author
Jeffrey.Stansbury@ucdenver.edu

Notes
The authors declare no competing financial interest.

ACKNOWLEDGMENTS

REFERENCES

(1) Shih, H.-W.; Vander Wal, M. N.; Grange, R. L.; MacMillan, D. W. C. *J. Am. Chem. Soc.* **2010**, *132*, 13600–13603.
(2) Hawker, C. J.; Wooley, K. L. *Science* **2005**, *309*, 1200–1205.
(3) Kilambi, H.; Reddy, S. K.; Schneidewind, L.; Stansbury, J. W.; Bowman, C. N. *Polymer* **2007**, *48*, 2014–2021.
(4) Hoyle, C. E.; Bowman, C. N. *Angew. Chem., Int. Ed.* **2010**, *49*, 1540–1573.
(5) Adzima, B. J.; Tao, Y.; Kloxin, C. J.; DeForest, C. A.; Anseth, K. S.; Bowman, C. N. *Nat. Chem.* **2011**, *3*, 256–259.
(6) Xuan, J.; Xiao, W.-J. *Angew. Chem., Int. Ed.* **2012**, *51*, 6828–6838.
(7) Narayanam, J. M. R.; Stephenson, C. R. J. *Chem. Soc. Rev.* **2010**, *40*, 102.
(8) Dai, C.; Narayanam, J. M. R.; Stephenson, C. R. J. *Nat. Chem.* **2011**, *3*, 140–145.
(9) Lee, T. Y.; Roper, T. M.; Jonsson, E. S.; Guymon, C. A.; Hoyle, C. E. *Macromolecules* **2004**, *37*, 3659–3665.
(10) Fors, B. P.; Hawker, C. J. *Angew. Chem., Int. Ed.* **2012**, *51*, 8850–8853.
(11) Wang, J.-S.; Matyjaszewski, K. *J. Am. Chem. Soc.* **1995**, *117*, 5614–5615.
(12) Yoon, T. P.; Ischay, M. A.; Du, J. *Nat. Chem.* **2010**, *2*, 527–532.
(13) Allonas, X.; Lalevée, J.; Fouassier, J. P. *J. Photochem. Photobiol., A* **2003**, *159*, 127–133.
(14) Fouassier, J. P.; Lalevée, J. *Photoinitiators for Polymer Synthesis: Scope, Reactivity, and Efficiency*, 1st ed.; Wiley-VCH: Weinheim, Germany, 2012.
(15) Fouassier, J.-P.; Morlet-Savary, F. *Opt. Eng.* **1996**, *35*, 304–312.
(16) EATON, D. *Science* **1991**, *253*, 281–287.
(17) Scott, T. F.; Kowalski, B. A.; Sullivan, A. C.; Bowman, C. N.; McLeod, R. R. *Science* **2009**, *324*, 913–917.
(18) Liu, N.; Liu, H.; Zhu, S.; Giessen, H. *Nat. Photonics* **2009**, *3*, 157–162.
(19) Goodner, M. D.; Bowman, C. N. *Chem. Eng. Sci.* **2002**, *57*, 887–900.
(20) Catilaz Simonin, L.; Fouassier, J. P. *J. Appl. Polym. Sci.* **2001**, *79*, 1911–1923.
(21) Stansbury, J. W. *J. Esthet. Dent.* **2000**, *12*, 300–308.
(22) Fisher, J. P. J.; Dean, D. D.; Mikos, A. G. A. *Biomaterials* **2002**, *23*, 4333–4343.
(23) DeForest, C. A.; Polizzotti, B. D.; Anseth, K. S. *Nat. Mater.* **2009**, *8*, 659–664.
(24) Hasenwinkel, J. M.; Lautenschlager, E. P.; Wixson, R. L.; Gilbert, J. L. *J. Biomed. Mater. Res.* **1999**, *47*, 36–45.
(25) Nakos, S. T.; Lin, S. Q. S. Dual curing coating method for substrates with shadow areas. U.S. Patent 4,699,802, October 13, 1987.
(26) Kwon, T.-Y.; Bagheri, R.; Kim, Y. K.; Kim, K.-H.; Burrow, M. F. *J. Invest. Clin. Dent.* **2012**, *3*, 3–16.
(27) Nason, C.; Roper, T.; Hoyle, C.; Pojman, J. A. *Macromolecules* **2005**, *38*, 5506–5512.
(28) Gregory, S. Ultraviolet curable resin compositions having enhanced shadow cure properties. U.S. Patent 6,245,827, June 12, 2001.
(29) Gugg, A.; Gorsche, C.; Moszner, N.; Liska, R. *Macromol. Rapid Commun.* **2011**, *32*, 1096–1100.
(30) Crivello, J. V. *J. Polym. Sci., Part A: Polym. Chem.* **2007**, *45*, 4331–4340.
(31) Lalevée, J.; Tehfe, M.-A.; Morlet Savary, F.; Graff, B.; Dumur, F.; Gigmes, D.; Blanchard, N.; Fouassier, J. P. *Chimia* **2012**, *66*, 439–441.
(32) Tehfe, M.-A.; Lalevée, J.; Morlet-Savary, F.; Graff, B.; Blanchard, N.; Fouassier, J. P. *ACS Macro Lett.* **2012**, *1*, 198–203.
(33) Zhang, G.; Song, I. Y.; Ahn, K. H.; Park, T.; Choi, W. *Macromolecules* **2011**, *44*, 7594–7599.

(34) Padon, K. S.; Scranton, A. B. *J. Polym. Sci., Part A: Polym. Chem.* **2000**, *38*, 2057−2066.

(35) Kim, D.; Stansbury, J. W. *J. Polym. Sci., Part A: Polym. Chem.* **2009**, *47*, 3131−3141.

(36) Kim, D.; Stansbury, J. W. *J. Polym. Sci., Part A: Polym. Chem.* **2009**, *47*, 887−898.

(37) Kim, D.; Scranton, A. *J. Polym. Sci., Part A: Polym. Chem.* **2004**, *42*, 5863−5871.

(38) Pierre Fouassier, J.; Lalevée, J. *RSC Adv.* **2012**, *2*, 2621.

(39) Scholes, G. D.; Fleming, G. R.; Olaya-Castro, A.; van Grondelle, R. *Nat. Chem.* **2011**, *3*, 763−774.

(40) Kavarnos, G. J. In *Photoinduced Electron Transfer I*; Springer-Verlag: Berlin, Germany, 1990; pp 21−58.

(41) Stansbury, J. W.; Dickens, S. H. *Dent. Mater.* **2001**, *17*, 71−79.

(42) Mills, A.; Lawrie, K.; McFarlane, M. *Photochem. Photobiol. Sci.* **2009**, *8*, 421.

(43) Galagan, Y.; Hsu, S.-H.; Su, W.-F. *Sens. Actuators, B* **2010**, *144*, 49−55.

(44) Goodspeed, F. C.; Scott, B. L.; Burr, J. G. *J. Phys. Chem.* **1965**, *69*, 1149−1153.

(45) Kavarnos, G. J.; Turro, N. J. *Chem. Rev.* **2001**, *86*, 401−449.

(46) Kim, D.; Scranton, A. B.; Stansbury, J. W. *J. Polym. Sci., Part A: Polym. Chem.* **2009**, *47*, 1429−1439.

(47) Sirovatka Padon, K.; Scranton, A. B. *J. Polym. Sci., Part A: Polym. Chem.* **2000**, *38*, 3336−3346.

(48) Asmusen, S.; Arenas, G.; Cook, W. D.; Vallo, C. *Dent. Mater.* **2009**, *25*, 1603−1611.

(49) Eaton, D. F. *Dye Sensitized Photopolymerization*; Volman, D. H., Hammond, G. S., Gollnick, K., Eds. John Wiley & Sons, Inc.: Hoboken, NJ, 1986; Vol. *13*, pp 427−487.

(50) Kim, D.; Scranton, A. B.; Stansbury, J. W. *J. Appl. Polym. Sci.* **2009**, *114*, 1535−1542.

(51) Galagan, Y.; Su, W.-F. *J. Photochem. Photobiol., A* **2008**, *195*, 378−383.

(52) Impert, O.; Katafias, A.; Kita, P.; Mills, A.; Pietkiewicz-Graczyk, A.; Wrzeszcz, G. *Dalton Trans.* **2003**, 348−353.

(53) Dektar, J. L.; Hacker, N. P. *J. Org. Chem.* **1990**, *55*, 639−647.

(54) Munekage, Y.; Hashimoto, M.; Miyake, C.; Tomizawa, K.-I.; Endo, T.; Tasaka, M.; Shikanai, T. *Nature* **2004**, *429*, 579−582.

(55) Hertle, A. P.; Blunder, T.; Wunder, T.; Pesaresi, P.; Pribil, M.; Armbruster, U.; Leister, D. *Mol. Cell* **2013**, *49*, 511−523.

(56) Datta, P.; Efimenko, K.; Genzer, J. *Polym. Chem.* **2012**, *3*, 3243.

(57) Mathew, J.; Mahadevan, V. *Macromol. Chem. Phys.* **1996**, *197*, 367−374.

(58) Chai, J.-D.; Head-Gordon, M. *Phys. Chem. Chem. Phys.* **2008**, *10*, 6615.

(59) Li, H.; Jensen, J. H. *J. Comput. Chem.* **2004**, *25*, 1449−1462.

(60) Zhao, Y.; Truhlar, D. G. *Theor. Chem. Acc.* **2007**, *120*, 215−241.

(61) Frisch, M. J.; Trucks, G. W.; Schlegel, H. B.; Scuseria, G. E.; Robb, M. A.; Cheeseman, J. R.; Scalmani, G.; Barone, V.; Mennucci, B.; Petersson, G. A.; Nakatsuji, H.; Caricato, M.; Li, X.; Hratchian, H. P.; Izmaylov, A. F.; Bloino, J.; Zheng, G.; Sonnenberg, J. L.; Hada, M.; Ehara, M.; Toyota, K.; Fukuda, R.; Hasegawa, J.; Ishida, M.; Nakajima, T.; Honda, Y.; Kitao, O.; Nakai, H.; Vreven, T.; Montgomery, J. A., Jr.; Peralta, J. E.; Ogliaro, F.; Bearpark, M.; Heyd, J. J.; Brothers, E.; Kudin, K. N.; Staroverov, V. N.; Kobayashi, R.; Normand, J.; Raghavachari, K.; Rendell, A.; Burant, J. C.; Iyengar, S. S.; Tomasi, J.; Cossi, M.; Rega, N.; Millam, N. J.; Klene, M.; Knox, J. E.; Cross, J. B.; Bakken, V.; Adamo, C.; Jaramillo, J.; Gomperts, R.; Stratmann, R. E.; Yazyev, O.; Austin, A. J.; Cammi, R.; Pomelli, C.; Ochterski, J. W.; Martin, R. L.; Morokuma, K.; Zakrzewski, V. G.; Voth, G. A.; Salvador, P.; Dannenberg, J. J.; Dapprich, S.; Daniels, A. D.; Farkas, Ö.; Foresman, J. B.; Ortiz, J. V.; Cioslowski, J.; Fox, D. J. *Gaussian 09*, revision D.01; Gaussian, Inc.: Wallingford, CT, 2009.

(62) Schmidt, M. W.; Baldridge, K. K.; Boatz, J. A.; Elbert, S. T.; Gordon, M. S.; Jensen, J. H.; Koseki, S.; Matsunaga, N.; Nguyen, K. A.; Su, S.; Windus, T. L.; Dupuis, M.; Montgomery, J. A. *J. Comput. Chem.* **1993**, *14*, 1347−1363.